Optimizing Electric Force for RF Blackout Mitigation

Anthony Corso - *Stanford University, Stanford, Ca, 94305*

Re-entry communications blackout has been a problem without a universally accepted solution since the early days of space exploration. Recently, however, a new approach known as Pulsed Electrostatic Manipulation (PEM) has shown promising progress towards mitigating the problem. This paper shows how PEM can be modeled using a 1D poisson equation with a known charge distribution. Once the model is created, the efficacy of PEM is optimized with respect to the electric permittivity of the plasma. A new optimization approach – a variation on a genetic algorithm – is shown to be more effective than a traditional conjugate gradient approach. The new optimization approach demonstrates that changing the permittivity in the plasma can have a large effect on the efficacy of PEM.

I. Introduction

This paper discusses the optimization of a design for a new method of mitigating the problem of re-entry communications blackout. It also proposes a new, modified genetic algorithm to optimize this design more efficiently as compared to traditional techniques. The remainder of this section provides background to the re-entry blackout problem as well as a model for a mitigation technique that suggests an objective function which can be optimized. Section II describes how the objective function can be computed numerically. Section III describes the optimization algorithms used, section IV displays the results of the optimization and section V concludes with a look at future work.

I.A. Background

Re-entry radio-communications blackout has been a problem since the early days of space exploration. The phenomenon occurs when a vehicle flies at hypersonic speeds – such as a spacecraft reentering Earth's atmosphere – and a plasma sheath forms around the vehicle which reflects or absorbs radiation in the radio-frequency band, effectively blocking all communication between the vehicle and the ground. The communications blackout restricts the amount of telemetry data that can be gained during reentry and is one of the many problems that needs to be solved for the development of other types of hypersonic vehicles[1].[2]

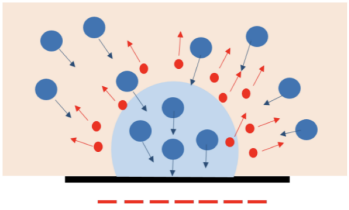

Figure 1. PEM reduces electron density to allow for communication. The red dotted line is the electrode, the black line is a dielectric, the blue dots are ions and the red dots are electrons.

In general, the higher the plasma density around the vehicle, the larger attenuation is seen at the common communication frequencies. To solve the reentry blackout problem then, the density of the plasma sheath needs to be reduced. One technique that has shown some promise at reducing plasma density is known as pulsed electrostatic manipulation (PEM).[1] In PEM, an electrode is installed in the surface of the space craft which emits a strong electric field into the plasma sheath. The electric field ejects the more light-weight electrons away from the region above the electrode, reducing the plasma density there. The effectiveness of these electrodes depends on many design parameters, including but not limited to:

- The size and shape of the electrode
- The magnitude and duration of the electric potential applied to electrode
- The composition of the material between the electrode and the plasma
- The number of electrodes and their placement on the vehicle

In order to arrive at an optimal solution, a design will have to consider all of these parameters. For the purposes of this project, however, only the composition of the material between the electrode and the plasma will be studied.

I.B. Model and Objective

In order to simplify the problem further, the time-dependent dynamics of the plasma will be ignored as will the the effects of magnetism. With this assumption, the electric field from the electrode will be governed by Poisson's equation which depends only on the permittivity ϵ and charge density ρ of the medium. Additionally, the domain will be reduced to 1D – spanning from the spacecraft surface out into plasma sheath. The charge density profile in this domain comes from the behavior of the plasma when the electric field is applied. Common profiles have been found through through simulation[1] and theory.[3] This leaves the permittivity as the parameter that can be used as the design variable.

The permittivity of a plasma is a complicated property that is governed by a diverse range of physical processes such as the frequency the incoming electromagnetic field, the collisional rate (both neutral and Coulombic), and the density of the plasma.[3] Although the permittivity cannot be adjusted directly in the region that the plasma occupies, properties of the plasma can be chosen through the location of the electrode on the vehicle, the vehicle geometry and the injection of material into the plasma sheath.[2] All of these control points can potentially be used to choose the permittivity profile of the re-entry plasma above the electrode. Putting the exact mechanism of control aside, however, this design process is focused on determining the optimal function of ϵ in the plasma domain.

The goal of the optimization is to maximize the number of negatively-charged electrons that will be ejected away from the electrode via a negative electric field. This can be achieved by minimizing the average electric field in the domain to the lowest possible negative value. It is also important to consider that, in a reentry plasma sheath, the plasma density is highest near the surface of the vehicle[4] so a weighting factor should be included in the objective which prioritizes regions near the surface. With all this in mind, the optimization objective can be described by the following PDE-constrained optimization problem

$$\min_{\epsilon(x)} \; E_{\text{avg}} = \int_0^1 w(x)E(x)dx \tag{1}$$

$$\text{s.t.} \quad R(x) = \frac{\partial}{\partial x}\left(\epsilon(x)\frac{\partial \phi}{\partial x}\right) - \rho(x) = 0 \tag{2}$$

$$\epsilon(x) \geq 1 \tag{3}$$

$$E(x) = -\nabla\phi(x) \tag{4}$$

where the weighting $w(x) = 2(1-x)$ was chosen for simplicity and so the average over the domain was equal to 1. E_{avg} is the weighted-average objective, $R(x)$ is the PDE residual from Poisson's equation and (4) is the definition of an electric field. Note that the constraint $\epsilon(x) > 1$ is the only constraint on the range of values available to the design variable and is imposed by the laws of physics. The next section describes how this optimization problem can be solved numerically.

II. Objective Function Solution Technique

In order to solve for the objective function value for a given choice of ϵ, the charge density must be described, Poisson's equation must be solved (with prescribed boundary conditions) and the electric field must be computed and averaged over. This section describes how each of those steps was completed.

II.A. Charge Distributions

Four simple, yet physically significant, charge distributions were chosen for the optimization process and are described below as well as plotted in figure 2.

1. $\rho_{\text{sheath}} = \rho_0 \exp(-5x)$ is a typical plasma sheath.[3]
2. $\rho_{\text{linear}} = \rho_0(1-2x)$ is a model charge distribution after the pulse has been on for a short time.
3. $\rho_{\text{heaviside}} = 2\mathcal{H}(0.5-x) - 1$ is the electron "hole" due to the pulse in a quasi steady state.[1]
4. $\rho_{\text{sinusoid}} = \rho_0 \cos(2\pi x) + \rho_0/2$ could result from an oscillating field.

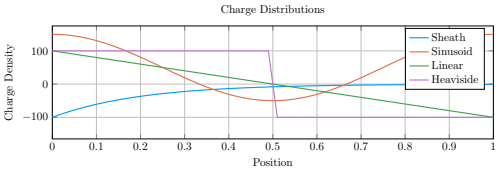

Figure 2. The charge densities

II.B. Numerical Solution of Poisson's Equation

Anticipating that the $\epsilon(x)$ that come out of the optimization process are not going to be analytic functions of x, a numerical solution technique should be employed to handle all types of input. To solve Poisson's equation numerically it must first be discretized onto a spatial 1D grid from $x = [0, 1]$ with N_g grid points. Start by expanding the derivative using the product rule and to get

$$\frac{\partial \phi}{\partial x}\frac{\partial \epsilon}{\partial x} + \epsilon(x)\frac{\partial^2 \phi}{\partial x^2} - \rho(x) = 0 \tag{5}$$

then discretize the equation by using the central difference approximation to the derivative

$$\frac{\partial \phi}{\partial x} \approx \frac{\phi_{i+1} - \phi_{i-1}}{2\Delta x} \qquad \text{and} \qquad \frac{\partial^2 \phi}{\partial x^2} \approx \frac{\phi_{i+1} - 2\phi_i + \phi_{i-1}}{\Delta x^2} \tag{6}$$

plugging these in to get

$$\left(\frac{\epsilon_{i+1} - \epsilon_{i-1}}{2\Delta x}\right)\frac{\phi_{i+1} - \phi_{i-1}}{2\Delta x} + \epsilon_i \frac{\phi_{i+1} - 2\phi_i + \phi_{i-1}}{\Delta x^2} - \rho_i = 0 \tag{7}$$

Then collect terms on the ϕ_i to get

$$\frac{1}{\Delta x^2}\left(\frac{1}{4}\epsilon_{i+1} + \epsilon_i - \frac{1}{4}\epsilon_{i-1}\right)\phi_{i+1} + \frac{1}{\Delta x^2}\left(-\frac{1}{4}\epsilon_{i+1} + a_i + \frac{1}{4}\epsilon_{i-1}\right)\phi_{i-1} - \frac{1}{\Delta x^2}2\epsilon_i\phi_i = \rho_i \tag{8}$$

or more compactly

$$d_{i+1,i}\phi_{i+1} + d_{i,i}\phi_i + d_{i-1,i}\phi_{i-1} = \rho_i \tag{9}$$

Assuming that $\rho(x)$ and $\epsilon(x)$ are prescribed and discretized into vectors, this equation can be written in matrix-multiplication form $D\vec{\phi} = \vec{\rho}$ where D is a matrix representing a differential operator whose coefficients are given by the expressions above for $d_{i,j}$. The matrix equation can be solved through the computation of D^{-1} and was computed, in this case, using Julia's backslash operator.

Likewise, the electric field was computed using finite differences (central difference in the middle of the domain and forward/backward difference on the boundaries) and the weighted average was computed with a summation

$$E_{\text{avg}} = \frac{1}{N}\sum_{1}^{N} 2(1 - x_i)E_i \tag{10}$$

II.C. Boundary Conditions

The boundary conditions of this problem are relatively straightforward. A fixed, strong negative potential is applied at the $x = 0$ boundary to simulate the spacecraft electrode. On the $x = 1$ boundary a potential of 0 is applied to simulate the plasma's tendency to shield out electric potentials and create net-zero potential in the bulk of the plasma. This leads to the following Dirichlet conditions at the 1D boundaries.

$$\phi_{x=0} = -1 \qquad \text{and} \qquad \phi_{x=1} = 0 \tag{11}$$

The potential is normalized to -1 for simplicity of computation.

To apply these boundary conditions, one can simply modify the system of equations to enforce these boundaries. This can be done by modifying the first and last rows of the matrix D and the RHS vector ρ. If d_i is the ith row of the matrix D then set

$$d_0 = \mathcal{I}_{\mathcal{N}(0)} \qquad \rho_0 = \phi_{x=0} \tag{12}$$

$$d_{N-1} = \mathcal{I}_{\mathcal{N}(N-1)} \qquad \rho_{N-1} = \phi_{x=1} \tag{13}$$

where $\mathcal{I}_{\mathcal{N}(i)}$ is the ith row of an $N \times N$ identity matrix. Note that the equations are assumed to be non-dimensionalized so there are no issues with units.

III. Optimization Algorithms

Two different optimization techniques were employed to solve this problem. This first is a modified genetic algorithm which uses physical domain knowledge to narrow the population of design variables to a sensible set of functions for better convergence and is described in section III.A. The second is an established first-order approach known as the conjugate gradient method and is described in section III.B.

III.A. Genetic Algorithm

Genetic algorithms (GA) are efficient methods for searching high-dimensional design spaces where gradient information is difficult to come by or there are many local minima in the objective function.[5] The basic algorithm starts with an initial population of individuals. The fittest individuals are given an opportunity to reproduce and create a new generation that has similar characteristics to the parents (using a process known as crossover) and then the individuals are mutated in order to introduce new characteristics into the gene pool.

Individuals in this problem are continuous 1D functions $\epsilon(x)$ which have been discretized onto a 1D grid. Given a continuous charge distribution (or a discontinuous one at a small number of points like a step function) it is expected that the optimal distribution of permittivity will be equally as continuous since they are related through a linear PDE. It therefore make sense to choose individuals that are smooth over the domain and mutations that tend to maintain their smoothness (instead of choosing random values at each grid point). With this smoothness consideration in mind the next several subsection describe the specifics of this new genetic algorithm.

III.A.1. Initial Population

Individuals are created using a combination of randomly sampled sinusoids of the form

$$\epsilon(x) = \sum_{i=1}^{m} A_i \sin(2\pi f_i x/L + \phi_i) \tag{14}$$

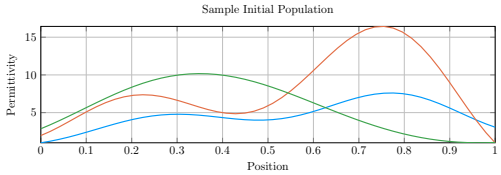

Figure 3. An initial population sample of 3 individuals

where m is the number of sinusoids to combine, $A_i \sim \mathcal{N}(0, \sigma_A)$ is the amplitude of the sinusoid, $f_i \sim \mathcal{N}(0, \sigma_f)$ is the sinusoid frequency, and $\phi_i \sim \mathcal{U}(0, 2\pi)$ is the phase shift, where $\mathcal{N}(\mu, \sigma)$ and $\mathcal{U}(v_{\min}, v_{\max})$ are the normal and uniform distributions, respectively. Three individuals from an example starting population are plotted in figure 3.

III.A.2. Parent Selection and Crossover

Parents were selected using Tournament Selection[5] where each parent was randomly selected from the fittest individuals. In particular, the population is sorted from lowest objective value to highest and then a particular fraction f_{elite} of the population is extracted and then randomly sampled from to produce the parents of a new generation that is the same size as the previous one.

When two parents are selected and create a new individual they employ a continuous crossover approach parameterized by a single variable λ. Two parents (ϵ_1 and ϵ_2) will create a new individual which has the values

$$\epsilon_{\text{new}} = \lambda\epsilon_1 + (1 - \lambda)\epsilon_2 \tag{15}$$

where $\lambda \sim \mathcal{U}(0, 1)$ is randomly chosen for each parental pairing.

III.A.3. Mutation

Before the end of each generation, each individual was mutated by having a random function ϵ_{mut} of the same form as equation 14 added to it. The frequency and phase shift come from the same distribution as the initial population while the amplitude $A_{\text{mut}} \sim \mathcal{N}(0, \sigma_{\text{mut}})$ has a separate standard deviation and the number of combined sinusoids m_{mut} may also be changed independently. ϵ_m is free to have a negative value in order to reduce the permittivty of the individual but a cutoff of $\epsilon \geq 1$ is ensured after the mutation is applied. A series of mutations is shown in figure 4. The new value of a mutated individual is given by

$$\epsilon^{(n+1)} = \max(1, \epsilon^{(n)} + \epsilon_m) \tag{16}$$

III.B. Conjugate Gradient Descent

The conjugate gradient descent method is a first-order technique that uses gradient information to iteratively get closer to the optimal design point.[5] Starting with a particular design point $\epsilon^{(0)}$, the first search direction $\vec{d}$ is found through the local gradient as $d^{(0)} = -\nabla f(x^{(0)})$. Then, the $k+1$ design point is found from the previous design point by

$$\vec{\epsilon}^{(k+1)} = \vec{\epsilon}^{(k)} + \alpha^{(k)}\vec{d}^{(k)} \tag{17}$$

where $\alpha^{(k)}$ is the optimal step size found using a line search in the direction $\vec{d}^{(k)}$. Future directions are chosen by a combination of the current gradient direction and the previous descent direction in an expression given by

$$\vec{d}^{(k+1)} = -\nabla f(x^{(k+1)}) + \beta^{(k)}\vec{d}^{(k)} \tag{18}$$

where $\beta^{(k)}$ was calculated using the Polak-Ribière[5][6] expression given by

$$\beta^{(k)} = \frac{\vec{d}^{(k)T}\left(\vec{d}^{(k)} - \vec{d}^{(k-1)}\right)}{\vec{d}^{(k-1)T}\vec{d}^{(k-1)}} \tag{19}$$

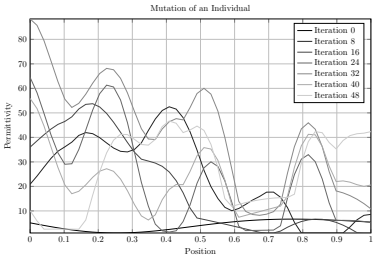

Figure 4. The mutation of an individual over 48 iterations. The black line represents the starting function of the individual. As the line gets lighter it corresponds to more mutations

In a PDE-constrained optimization problem it is often difficult to compute the gradient of an objective function with respect to the many design variables of interest. When computing the objective numerically, however, automatic differentiation (AD) (described here[5] and here[7]) can be employed to compute the gradient without much extra cost. For this implementation, the library `ReverseDiff.jl`[8] was used to employ reverse-mode AD to compute the gradients of the present objective function with respect to each discretized value of ϵ. Due to a performance cost of about $4\times$,[8] each computation of the gradient in the CG method will be counted as 4 function evaluations for comparison to the genetic algorithm.

IV. Results

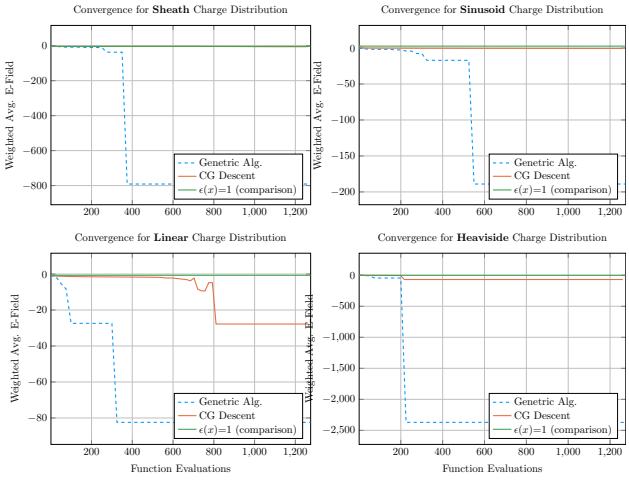

Figure 5. The convergence history for both algorithms

Both of the algorithms discussed above were implemented in the Julia language and were used to optimize the four charge distributions outlined in section II.A. For each charge distribution, each algorithm was given a fixed number of objective function evaluations (~ 1300) to find an optimal permittivity distribution in the domain which was discretized into $N_g = 50$ grid points. The final permittivity distribution and resulting electric field is plotted in figure 6. The history of the minimum objective function value is plotted in figure 5.

The hyper-parameters of the genetic algorithm were manually tuned to produce the best possible results. The stddev of the amplitude of the initial population and successive mutations was $\sigma_A = \sigma_{\text{mut}} = 10$, the stddev of the frequency was $\sigma_f = 0.03/\Delta x = 1.47$, the number of sinusoids combined for the initial population was $m_{\text{init}} = 5$ while the number combined for the mutation was $m_{\text{mut}} = 1$. The elite fraction of the population was $f_{\text{elite}} = 0.15$ while the population was maintained at $N_{\text{pop}} = 25$.

V. Conclusions and Future Work

It can be seen from the convergence history that the genetic algorithm outperforms the conjugate gradient method in all four cases that were investigated. In those cases, both algorithms identified similar broad regions of interest where the permittivity should be large. They both found a high negative electric field near $x = 0$ while allowing for positive fields near $x = 1$ where the weighting factor is smaller.

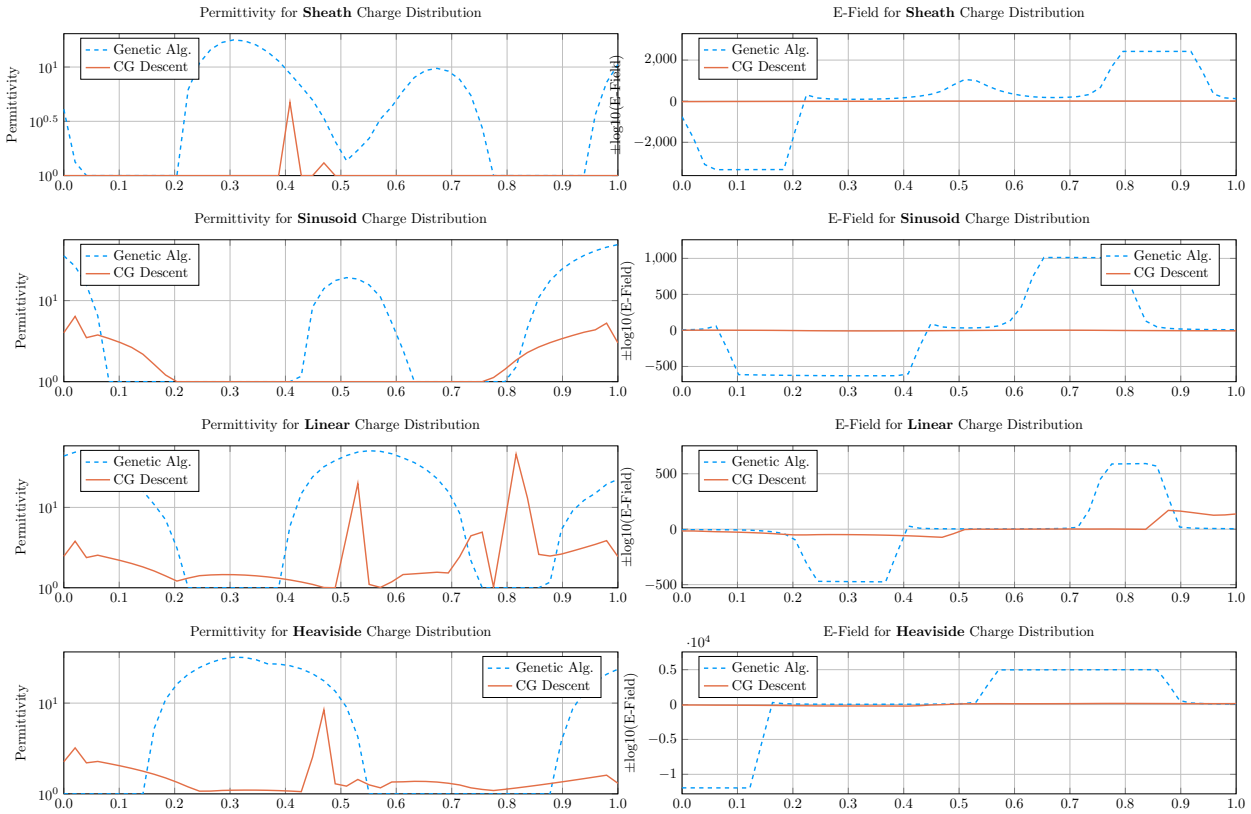

Figure 6. The optimal permittivity from both algorithms (left column) and the resulting electric field (right column)

There is a strong difference, however, in the relative smoothness and magnitude of the optimal permittivities. The genetic algorithm, by design, provided smoother solutions over a broader regions of the domain, while the conjugate gradient algorithm tended to favor sharper peaks. The genetic algorithm was also able to reach large permittivity values across the domain while the conjugate gradient was forced to take small steps and often didn't exceed a permittivity of $\epsilon = 10$ outside of the one or two spikes in each domain. Additionally, it was observed that the CG method reached a local minimum in two of the four cases while the genetic algorithm, due to its volatility, appeared to be able to search around local minima and found minimizers that were far better than those reached by the conjugate gradient method.

Future work in this field would include further tuning of the hyper-parameters, trying other smooth basis functions, and expanding the analysis to multiple dimensions. Additionally, an investigation needs to be done into how much the permittivity can be actively controlled from the spacecraft. Lastly, all of the other design variables should be included in a full optimization of PEM.

References

[1]Krishnamoorthy, S. and Close, S., "Investigation of plasmasurface interaction effects on pulsed electrostatic manipulation for reentry blackout alleviation," *Journal of Physics D: Applied Physics*, Vol. 50, No. 10, 2017, pp. 105202.

[2]Rybak, J. P. and Churchill, R. J., "Progress in Reentry Communications," *IEEE Transactions on Aerospace and Electronic Systems*, Vol. AES-7, No. 5, 1971, pp. 879–894.

[3]Francis, F., "Introduction to Plasma Physics and Controlled Fusion," *Plasma Physics*, 1984.

[4]Evans, J., Schexnayder, C., and Huber, P. W., "Boundary Layer Electron Profiles for High-Altitude Entry of a Blunt Slender Body," *AIAA Journal*, Vol. 11, No. 10, 1973, pp. 1371–1372.

[5]Kochenderfer, M. and Wheeler, T., *Algorithms for Optimization*, 2017.

[6]Societe de mathematiques appliquees et industrielles., E. and Ribiere, G., *Mathematical modelling and numerical analysis = Modelisation mathematique et analyse numerique.*, Vol. 3, EDP Sciences.

[7]Carpenter, B., Hoffman, M. D., Brubaker, M., Lee, D., Li, P., and Betancourt, M., "The Stan Math Library: Reverse-Mode Automatic Differentiation in C++," sep 2015.

[8]Revels, J., "ReverseDiff.jl," 2016.